

## Inversion of surface composition and evolution of nanostructure in Cu/Co nanocrystals

A. S. Edelstein,<sup>a)</sup> V. G. Harris, D. R. Rolison, and L. Kurihara  
*Naval Research Laboratory, Washington, DC 20375*

David J. Smith

*Department of Physics and Astronomy and Center for Solid State Science, Arizona State University,  
 Tempe, Arizona 85287*

J. Perepezko and M. H. da Silva Bassani

*Department of Materials Science and Engineering, University of Wisconsin, Madison, Wisconsin 53706*

(Received 7 December 1998; accepted for publication 25 March 1999)

Nanocrystals of Cu/Co with a nearly pure Cu core and a Co-rich shell have been chemically synthesized. This structure results from reaction kinetics and represents an inversion of surface composition since the surface energy of Co is larger than that of Cu. Both the Cu core and the Co-rich shell initially have an fcc structure and a common lattice constant. Annealing at temperatures in the range of 300 to 600 °C causes the material to phase separate, forming small, increasingly pure Co nanocrystals which aggregate on the surface of the pure Cu nanocrystals. © 1999 American Institute of Physics. [S0003-6951(99)02621-2]

The Cu/Co system, which has no intermetallic compounds and limited mutual solubility, has been studied extensively.<sup>1,2</sup> Despite the limited solubility, metastable solid solutions have been prepared by rapid quenching,<sup>2,3</sup> sputtering,<sup>4,5</sup> and mechanical attrition.<sup>6,7</sup> Giant magnetoresistance in granular systems was first observed<sup>5,8</sup> in phase-separated, sputtered films of Cu<sub>8</sub>Co<sub>2</sub>.

Here we report the chemical synthesis of nanocrystalline Cu<sub>80</sub>Co<sub>20</sub> with an unusual structure. The nanocrystals have a nearly pure Cu face-centered-cubic (fcc) core and a Co-rich outer fcc shell with the same lattice constant as the Cu core. This result is surprising because the surface energy<sup>9</sup> of Cu, 1.934 J m<sup>-2</sup>, being smaller than that of Co, 2.709 J m<sup>-2</sup>, affects the morphology of Cu/Co bilayers. For example, a 380 K anneal of a thin Co film deposited on Cu causes Cu atoms to diffuse through pinholes onto the Co surface.<sup>10</sup> Our surface composition inversion is a result of reaction kinetics.

Annealing causes the material to phase separate, forming smaller, increasingly pure, Co nanocrystals which form on the surface of the larger, pure Cu nanocrystals. A potentially useful property of the material is that because the Co oxidizes preferentially, the oxidation of the Cu is significantly delayed.<sup>11</sup> The polyol process is another chemical route that has been used<sup>12</sup> to investigate nanocrystalline Cu/Co, but no evidence was found for the structural evolution reported here.

Our material is prepared by first precipitating a hydroxide from solutions of either metallic chlorides or nitrates. The hydroxide is converted first to an oxide and then reduced to metallic form (flowing hydrogen at 205–215 °C for 15 min). Heat treatments at higher temperatures and longer times cause complete phase separation and increase the particle size. The different stages of the structural evolution are illustrated in Fig. 1. It is important that one or both of the

precursors, the hydroxide and/or the oxide, contains a mixture of Cu and Co. If not, then reduction leads directly to phase separation. When we apply a similar procedure to the Cu/Fe system, a metastable solid solution is not formed (presumably because Cu and Fe do not form mixed metal precursors). In the following, we present experimental evidence supporting the structural and morphological evolution described above.

X-ray photoelectron (XPS) and energy-dispersive x-ray (EDXS) spectroscopy measurements provide evidence for the composition inversion, i.e., that Co-rich regions reside on the surface of the Cu nanocrystals. XPS measurements, which probe only the only first few atomic layers from the surface, show Co to Cu ratios of 1.15 and 0.40±0.02, respectively, for samples heat treated for 15 min at 215 and 600 °C. Thus, the Co concentration is enhanced near the surface by factors of approximately four and two at these temperatures.

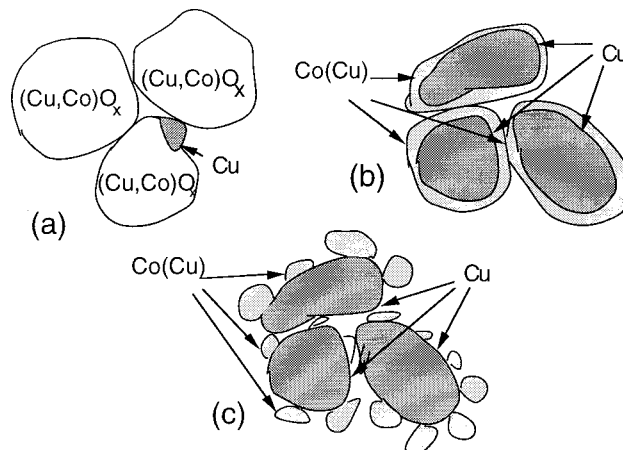


FIG. 1. Schematic of nanostructural evolution, (a)–(c), as chemically synthesized Cu/Co is reduced and heat treated in flowing H<sub>2</sub>.

<sup>a)</sup>Electronic mail: edelstein@anvil.nrl.navy.mil

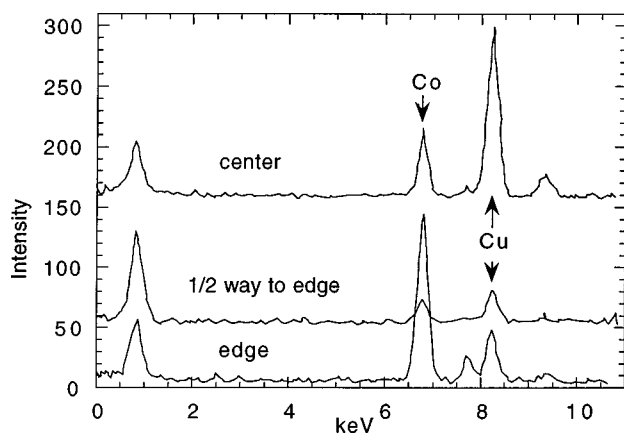


FIG. 2. Series of energy-dispersive x-ray spectra from agglomerate of phase-separated nanocrystalline  $\text{Cu}_{80}\text{Co}_{20}$  heated to  $600^\circ\text{C}$  showing the variation in relative Cu and Co concentrations as a 1 nm probe was moved from the center, to between the center and the edge, and to the edge of the agglomerate.

Presumably, the enhancement is smaller for the  $600^\circ\text{C}$  sample because the Co-rich regions ball-up during phase separation when they form crystals on the nanocrystalline Cu surfaces and interfaces. This balling-up is similar to the island formation that occurs during the initial stage of film growth.

EDXS measurements, using a Philips 400 ST-FEG (100 keV, 1 nm probe) were undertaken on nanocrystalline agglomerates of the phase-separated material. The relative Cu and Co concentrations in a sample heated to  $600^\circ\text{C}$  as a function of position were inferred from these measurements by the height variations of the Cu and Co peaks shown in Fig. 2. The Co:Cu ratio increases as the probe is moved from the center to the edge of the agglomerate, with the highest Co concentration occurring when the probe was located on or very close to a small particle at the very edge. This result supports the description of the microstructure shown in Fig. 1(c).

X-ray diffraction (XRD) measurements (Cu  $K\alpha$  radiation) on samples of  $\text{Cu}_{1-x}\text{Co}_x$  ( $x=0.2$  and  $0.4$ ), reduced in flowing hydrogen for 15 min at  $215^\circ\text{C}$ , show a single set of fcc diffraction peaks. The lattice parameters derived by XRD for these Cu/Co samples are shown in Fig. 3. The values deviate from Vegard's law but are in general agreement with those obtained from vapor quenched samples<sup>13</sup> and for meta-

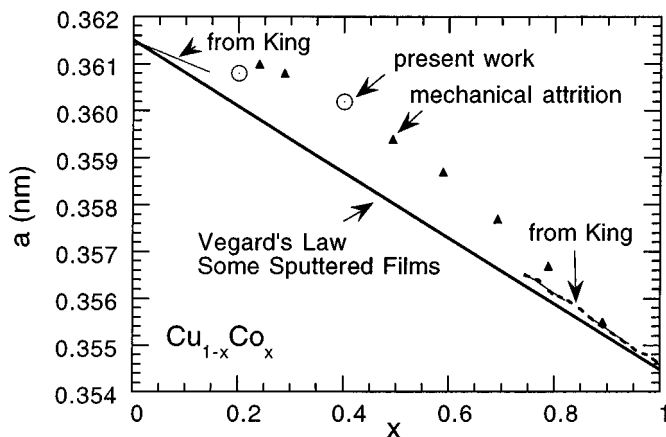


FIG. 3. Lattice constant of solid solutions of  $\text{Cu}_{1-x}\text{Co}_x$  vs.  $x$ .

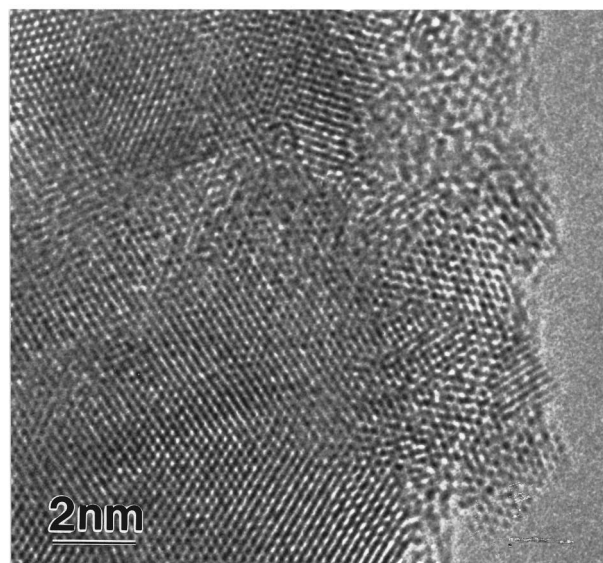
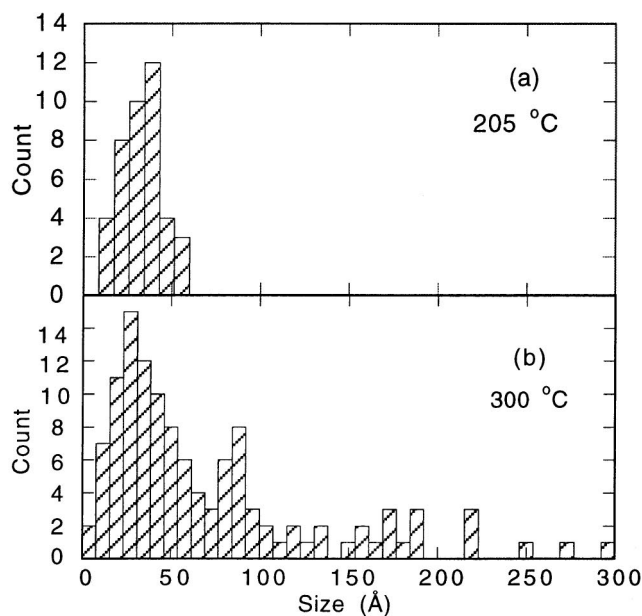


FIG. 4. Histograms of particle size obtained from high-resolution transmission electron micrographs taken on nanocrystalline  $\text{Cu}_{80}\text{Co}_{20}$  samples heat treated at: (a)  $205^\circ\text{C}$  and (b)  $300^\circ\text{C}$ . (c) High resolution electron micrograph from  $\text{Cu}_{80}\text{Co}_{20}$  annealed at  $300^\circ\text{C}$  showing nanocrystallites decorating surfaces of larger crystalline particles.

stable solid-solution samples prepared by mechanical attrition.<sup>7</sup> When higher annealing temperatures ( $T > 250$ – $300^\circ\text{C}$ ), are employed, two sets of fcc XRD peaks are observed. One set corresponds to the unit-cell constant of Cu, 0.3615 nm. The other set corresponds to a smaller value which decreases with increasing annealing temperature and approaches the value for fcc Co. Thus, the Co or Co-rich regions retain an fcc structure but do not have the same lattice constant as the Cu regions, implying the presence of incoherent interfaces.

High-resolution transmission electron micrographs were recorded with a JEM-4000EX high-resolution electron microscope to determine the particle size distribution,  $p(r)$ , of two  $\text{Cu}_{80}\text{Co}_{20}$  samples annealed for 1 h at 205 and  $300^\circ\text{C}$ . These distributions are shown in Figs. 4(a) and 4(b), respectively. The distribution  $p(r)$  has a single peak for the  $205^\circ\text{C}$

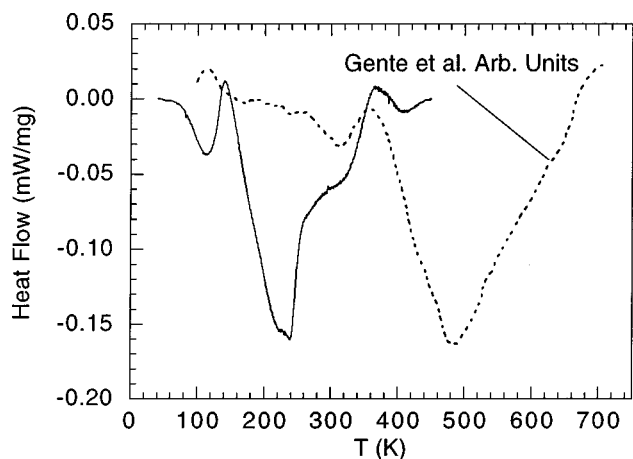


FIG. 5. Comparison of the exotherm in DSC measurements on nanocrystalline  $\text{Cu}_{80}\text{Co}_{20}$  previously reduced at  $205\text{ }^{\circ}\text{C}$  with the exotherm observed in DSC measurements on metastable  $\text{Cu}_{50}\text{Co}_{50}$  solid solutions made by mechanical attrition (Ref. 7).

sample, but two peaks are visible for the  $300\text{ }^{\circ}\text{C}$  sample. These two peaks presumably represent the sizes of the pure Cu crystals and the smaller Co-rich crystals formed after phase separation has occurred. A volume estimate, using the  $r$  values shown in Figs. 4(a) and 4(b), indicates that the larger  $r$  peak represents particles with approximately four times the volume of the particles corresponding to the smaller  $r$  peak. This result is consistent with the smaller  $r$  peak being due to the Co-rich nanocrystals. The typical morphology observed for the  $300\text{ }^{\circ}\text{C}$  sample is shown in Fig. 4(c), where nanocrystallites decorate surfaces of larger crystalline particles.

The composition of the particles as a function of heat treatment, as estimated from the lattice parameter determined by XRD is consistent with the Co-rich regions becoming purer as the sample is heated to  $600\text{ }^{\circ}\text{C}$ . The question arises whether the single set of fcc x-ray diffraction peaks observed for the sample annealed at  $215\text{ }^{\circ}\text{C}$  is due solely to a small crystallite size which would cause peak broadening. This explanation seems unlikely since two sets of fcc x-ray diffraction peaks are observed for the sample annealed at  $300\text{ }^{\circ}\text{C}$ , which contains even smaller crystals.

Differential scanning calorimetry (DSC) measurements, using a heating rate of  $20\text{ }^{\circ}\text{C}/\text{min}$ , were performed on a sample of  $\text{Cu}_{80}\text{Co}_{20}$  that had been reduced for 15 min in flowing hydrogen at  $215\text{ }^{\circ}\text{C}$ . The heat given off is compared in Fig. 5 with the exotherm observed in DSC measurements, using the same heating rate, on metastable  $\text{Cu}_{50}\text{Co}_{50}$  solid solutions made by mechanical attrition.<sup>7</sup> Although the two exotherms are similar, there are important differences. The exotherm in our experiment occurs at lower temperatures and has sharper features. The large temperature shift is probably due to the fact that our nanocrystals are approximately a factor of ten smaller than those of Gente, Oehring, and Bormann<sup>7</sup> and, hence, in phase separating, the atoms have less distance to diffuse. The area under the Gente, Oehring, and Bormann isotherm and under our isotherm indicates that the heat released is 12.0 and 3.26 kJ/g atom, respectively. Our value is approximately ten times as large as our estimate of the maximum energy that could be stored as elastic energy if the sample were already phase separated. This estimate is

based on the lattice constant of the sample and the bulk moduli of Cu and Co. This large energy release supports our claim that the sample prepared at  $215\text{ }^{\circ}\text{C}$  was an inhomogeneous, metastable, solid solution. The energy given off is consistent with the Co-rich regions containing 40% Cu.

Atoms on the surfaces and at the interfaces of the hydroxide/oxide crystals will be the first to be reduced to their metallic state. Cu crystals will nucleate and grow first, as depicted in Fig. 1(a), because there are more Cu than Co atoms and because Cu is thermodynamically more easily reduced than Co to its metallic state. The remaining material will become increasingly Co rich. Two alternatives for what will happen as further atoms are reduced to their metallic state are: (1) as the Cu crystals grow, separate Co crystals nucleate on the Cu with incoherent interfaces; and (2) the Co-rich atoms are incorporated onto the surface of the Cu crystals that are already present [Fig. 1(b)]. Our work suggests that initially the second alternative occurs. It appears that annealing then causes the material to phase separate, forming smaller, increasingly pure, Co nanocrystals which form on the surfaces of the larger, pure Cu nanocrystals [Fig. 1(c)].

In summary, we have presented experimental results using several techniques which support the unusual, nanostructural evolution of chemically synthesized Cu/Co nanostructures illustrated in Fig. 1. The x-ray photoelectron, high-resolution electron micrographs, and nanoprobe x-ray spectra provide direct evidence in support of this scenario.

Conversation with S. P. Marsh and the financial support of the Office of Naval Research are gratefully acknowledged. Electron microscopy was undertaken at the Center for High Resolution Electron Microscopy at Arizona State University supported by the National Science Foundation Grant No. DMR-9314326. The authors thank K. Weiss for assistance with acquisition of x-ray spectra.

- <sup>1</sup>Y. Nakagawa, *Acta Metall.* **6**, 704 (1958).
- <sup>2</sup>R. Busch, F. Gärtner, C. Borchers, P. Haasen, and R. Bormann, *Acta Metall. Mater.* **43**, 3467 (1995).
- <sup>3</sup>J. Wecker, R. von Helmholt, L. Schultz, and K. Samwer, *Appl. Phys. Lett.* **62**, 1985 (1993).
- <sup>4</sup>J. R. Childress and C. L. Chien, *Phys. Rev. B* **43**, 8089 (1991).
- <sup>5</sup>A. W. Berkowitz, J. R. Mitchell, M. J. Carey, A. P. Young, S. Zhang, F. E. Spada, F. T. Parker, A. Hutten, and G. Thomas, *Phys. Rev. Lett.* **68**, 3745 (1992).
- <sup>6</sup>M. Baricco, N. Cowlam, L. Schiffini, P. P. Macri, R. Frattini, and S. Enzo, *Philos. Mag. B* **68**, 957 (1993).
- <sup>7</sup>C. Gente, M. Oehring, and R. Bormann, *Phys. Rev. B* **48**, 13244 (1993).
- <sup>8</sup>J. Q. Xiao, J. Samuel Jiang, and C. L. Chien, *Phys. Rev. Lett.* **68**, 3749 (1992).
- <sup>9</sup>M. A. Turchanin, *Russ. Metall.* **5**, 9 (1995).
- <sup>10</sup>M. Giesen, F. Schmitz, and H. Ibach, *Surf. Sci.* **336**, 269 (1995).
- <sup>11</sup>F. H. Kaatz, V. G. Harris, L. Kurihara, D. R. Rolison, and A. S. Edelstein, *Appl. Phys. Lett.* **67**, 3807 (1995).
- <sup>12</sup>G. M. Chow, L. K. Kurihara, K. M. Kemner, P. E. Schoen, W. T. Elam, A. Ervin, S. Keller, Y. D. Zhang, J. Budnick, and T. Ambrose, *J. Mater. Res.* **10**, 1546 (1995).
- <sup>13</sup>H. W. King, *J. Mater. Sci.* **1**, 79 (1966).